Mater. Res. Soc. Symp. Proc. Vol. 960 © 2007 Materials Research Society 0960-N03-03

Control of Growth and Morphology of a Crystal Surface by Induced Spatio-Temporal Oscillations of Surface Temperature

Mikhail Khenner
Mathematics, State University of New York at Buffalo, College of Arts and Sciences, 244 Mathematics Bldg., Buffalo, NY, 14260

ABSTRACT

This paper presents the model for pattern formation in the course of thermodynamically stable and unstable crystal growth from vapor phase, which is influenced by rapid spatio-temporal variations of substrate and film temperature. In the model, such variations result from the interference heating of a substrate by weak pulsed laser beams. In the thermodynamically stable case the surface relaxational dynamics is influenced by surface diffusion mass transport from hot to cold regions of a substrate; this leads to accumulation of mass in cold regions and depletion in hot regions. In the thermodynamically unstable case the underlying faceting (spinodal) instability coupled to diffusion mass fluxes from hot to cold regions leads to formation of pyramidal surface structures. The scale of stationary coarsened structure increases as the separation distance of the adjacent interference fringes decreases (relative to the intrinsic faceting wave length, which is determined by the balance between the corner regularization energies and the surface energy anisotropy). On the other hand, the coarsening rates decrease with decreasing the separation distance, at least at particular typical deposition strength. The deposition strength and the separation distance of the interference fringes determine the transient and stationary pattern shape. By effectively redistributing adatoms on a substrate through the enhanced, spatially inhomogeneous diffusion, the interference heating mechanism delays, for large separation distances, the onset of spatiotemporal chaos as the growth rate increases.

INTRODUCTION

Recent experimental work done in the group of Ramki Kalyanaraman at Washington University [1]-[3] demonstrates that temperature field could be used to engineer morphologies. These researchers observed spatial organization of structures on growing surfaces of thin solid films irradiated by weak, pulsed laser beams that are made to interfere on a substrate. It was suggested that the non-isothermal surface diffusion resulting from the rapid spatio-temporal variations of the surface temperature is the cause of pattern formation.

It is well-known that on thermodynamically unstable crystal surfaces structures are formed by the combined action of the deposition, faceting instability and coarsening of faceted domains [4]-[6]. Thus the proposed model for morphology evolution in the presence of weak spatial non-uniformity of the surface heating is formulated in terms of regularized, unstable evolutionary partial differential equation (PDE). The interference heating is factored in through Arrhenius dependence of the adatom diffusivity on temperature, and manifests in space-dependent coefficients (temperature dependence of the surface energy anisotropy can be included in a similar fashion). The evolutionary PDE can be reduced to high-order, convective Cahn-Hilliard equation in the special case of constant temperature and after long wave length approximation. The proposed model allows morphological evolution studies of two-dimensional surfaces as a function of external parameters, such as the separation distance of the interference fringes, interference strength, radiation power intensity and surface absorptivity.

THEORY

Considered is a 1+1 case corresponding to a two-dimensional crystal with a one-dimensional surface. The evolution of the crystal surface $z = h(x\ t)$ is described by the following mass conservation PDE [7]-[10]:

$$h_t = F\ \ \overline{1 + h_x^2} + A\overline{x}\ \ \frac{\exp\left(-E_d\ \ kT\right)}{kT}(1 + h_x^2)^{-1\ \ 2}\overline{x}\kappa W(\theta\ \ \kappa) \tag{1}$$

where all subscripts denote differentiation, F is vertical rate of growth of the planar surface ($h_x = 0$) by deposition along the normal (typical to vapor-phase growth), $A = \Omega^2 \nu D_0 \gamma_0$, κ is the curvature and [11]

$$W(\theta\ \ \kappa) = 1 - 15\epsilon \cos 4\theta - \frac{\delta}{\gamma_0}\left(\frac{1}{2}\kappa^2 + \frac{\kappa_{ss}}{\kappa}\right) \tag{2}$$

In the Eq. (2) θ is the angle that the local unit normal to the crystal surface makes with the [01] crystalline direction, s is the arc length along the surface (note that $s = (1 + h_x^2)^{-1\ \ 2}\ \ x$), γ_0 is the energy of forming new vicinal surface of unit dimension and ϵ is the strength of the surface energy anisotropy $\gamma(\theta\ \ \kappa)$, see for instance Ref. [12] and references therein:

$$\gamma(\theta\ \ \kappa) = \gamma_0(1 + \epsilon \cos 4\theta) + \frac{\delta}{2}\kappa^2 \tag{3}$$

$\delta = const\ > 0$ is the small regularization parameter having units of energy. The dependence of the diffusivity on temperature is shown explicitly in the evolution Eq. (1). Other quantities have the usual meaning. The Eq. (1) is fourth-order when the anisotropy is weak ($\epsilon < 1\ \ 15$) and the regularization is not needed, e.g. $\delta = 0$ and sixth-order when the anisotropy is strong ($\epsilon \geq 1\ \ 15$) and the equation must be regularized.

Far from the melting threshold the pulsed laser irradiation gives rise to a quasistationary state in which the temperature of the irradiated section of a surface fluctuates about the mean value T_0 with a frequency of source pulse repetition. For metallic films, a quasistationary state is achieved often after as few as ten pulses. The heat conduction problem in films uniformly irradiated by laser pulses was solved in Refs. [13]-[15]. These results, as well as the experiments [13] describe the quasi-steady state on a surface and quantify transient temperature distributions. To this end, assume that the entire surface of the horizontal dimension L is irradiated.

Eq. (1) admits the trivial solution

$$h = h(t) = Ft + h_0 \qquad h_0 = const \tag{4}$$

at any temperature $T = T(x\ t)$. This solution corresponds to a crystal with the planar surface growing vertically at constant rate F. Without loss of generality the reference value h_0 can be chosen zero. Introduce the perturbation $h = h(x\ t)$ of the steady state (4), and the simultaneous perturbation of the mean temperature field, $T = T_0 + T(x\ t)$, such that $\left|T(x\ t)\ \ T_0\right| \equiv\ T(x\ t)\ \ll 1$.

To close the model, a realistic form for the temperature perturbation $T(x\ t)$ is required. The following is used in the 1+1 case:

$$T(x\ t) = (Q_0 \cos\ \ t)\,(1 + Q_1 \cos qx) \tag{5}$$

This form approximates well [3] the one-dimensional interference fringes from the two pulsed beams, which originate from a split single pulsed laser beam. $0 < Q_0 \ll 1$ determines the magnitude of small temporal oscillations about T_0 due to the pulsed nature of irradiation and $0 < Q_1 < 1$ determines the difference of the mean temperatures at regions (fringes) of constructive and destructive interference. Distance d between centers of two adjacent fringes is related to the angle that two beams form. If this angle is 2ϕ, then $d = 2\pi\ \ q = \quad (2\sin\phi)$, where $\quad$ is the wave length of a laser pulse [1]. Parameters $Q_0\ \ Q_1$ and the mean temperature T_0 are known functions of the radiation power intensity, surface absorptivity at the radiation wavelength, and the thermophysical and other optical characteristics of the material [13, 14].

To model the surface evolution on the long time scale associated with formation of experimentally detectable structures, it is sufficient to use the Eq. (1) where the coefficients that involve the temperature perturbation are averaged over the period of pulse repetition, $2\pi\quad$. In other words, the differentiation at the left hand side of the Eq. (1) is treated as being with respect to the slow time associated with the typical long time scale of morphological changes due to surface diffusion, while the form (5) involves the fast time associated with the short duration of a laser pulse. Averaging is with respect to the fast time during which the film height is constant. Finally, the Eq. (1) is nondimensionalized, expanded in powers of the small quantity T up to second order, and averaged:

$$h_t = f\left(-1 + \quad \overline{1 + h_x^2}\right) + B\frac{}{x}\ \ (1 + \alpha\ T^2\ )(1 + h_x^2)^{-1\ 2}\frac{}{x}\kappa W(\theta\ \ \kappa) \tag{6}$$

where $f = F\ \ (L\ \ )$, $B = A\exp(-E_d\ \ kT_0)\ \ (\ \ L^4 kT_0)$ and $\alpha = (E_d\ \ kT_0)^2\ \ 2 - 2E_d\ \ kT_0 + 1$. The form of $W(\theta\ \ \kappa)$ does not change upon non-dimensionalization, except $\delta\ \ \gamma_0$ in the Eq. (2) is replaced by $\Delta = \delta\ \ (\gamma_0 L^2)$. These parameters are positive. The Eq. (6) is written in the frame of reference moving in the z direction with the speed F, and the tilde sign over h is omitted. The averaged square of the temperature perturbation in the Eq. (6) is given by $\ T^2\ \ = Q_0^2\,(1 + Q_1 \cos 2\pi\bar{q}x)^2\ \ 2$, where the 2π-based scale for the non-dimensional wave number $\bar{q} = qL$ is adopted for convenience. Note that the Eq. (6) involves the coefficients that depend on the space coordinate, x. This makes analytical solution difficult and the numerical methods are preferred.

For computations, the discretization in space was implemented by the novel nested finite volume method, and the time-stepping was performed using the RADAU code, which is based on implicit Runge-Kutta methods with variable order (5, 9, 13) [17]. I showed in [16] that this numerical method is more robust than standard finite differences, and also much more accurate in computing faceting with large slopes, deposition, surface diffusion, and non-uniform heating.

RESULTS AND DISCUSSION

Case of isotropic surface energy ($\epsilon = 0$)

$\epsilon = 0$ implies $\Delta = 0$ and thus $W = 1$ in the Eq. (6) (see Eq. (2)). The faceting instability is absent and the initially present surface morphology slowly decays while the average surface height increases due to deposition. Interestingly, the non-uniformity of the surface temperature results in the non-uniformity of the decay rates along the surface. As an example of such morphology evolution, Figure 1 shows the relaxation of the cosine curve $z = 0\ 02 \cos 8\pi x$ for the case $\bar{q} = 2$ (thus the temperature maximum occurs at the first, third, and fifth (last) maxima of the surface, and the temperature minimum occurs at the second and fourth maxima of the surface). One can see coarsening of the perturbation - the material accumulates near $x = 0\ 25$ and $x = 0\ 75$ due to diffusive transport from the adjacent hotter regions near $x = 0\ \ 0\ 5$ and 1. This is exactly the mechanism Zhang & Kalyanaraman proposed as part of the explanation of their experimental data. The accumulation of material at colder regions results in slowly decaying surface spikes.

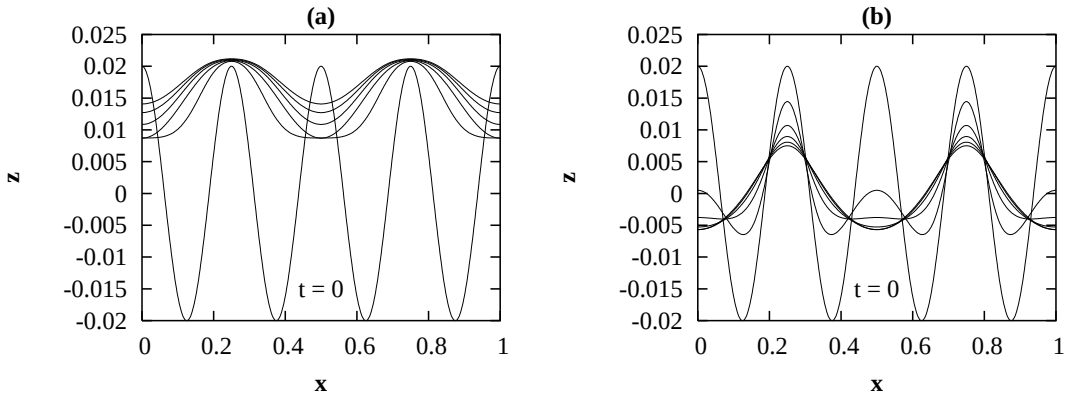

Figure 1: Relaxation of the perturbation in the thermodynamically stable case (e.g., surface energy isotropic) and when (separation distance of the interference fringes) = 2*(wave length of the surface perturbation). (a) $f = 10^{-6}$. (b) $f = 10^{-9}$. Other parameters are $B = 5 \times 10^{-13}$ $\alpha = 43$ $Q_0 = 0\ 5$ $Q_1 = 0\ 99$.

Case of strongly anisotropic surface energy ($\epsilon > 1\ \ 15$)

Values $\epsilon = 0\ 5$ and $\Delta = 0\ 0275$ were chosen for the simulations in this section. (Corresponding to these values, the wave length of the most unstable linear mode is $\lambda_{\max} = 2\pi\ \ 3\Delta\ \ 2\,(15\epsilon - 1) = 0\ 5$ [18]). The evolution of small amplitude random perturbation in the domain $0 \le x \le 20$ was computed for values of f in $[10^{-10}\ \ 10^{-6}]$ and $\bar{q}$ in $[0\ 25\ \ 8]$. Grid spacing is $\delta x = 0\ 02$.

Figures 2(a)-(f) show the surface shapes for different non-dimensional separation distance of the interference fringes $\bar{d} = 1\ \ \bar{q}$, where $\bar{q} = 0\ 25\ \ 0\ 5\ \ 1\ \ 2\ \ 4\ \ 8$, respectively. The surface shapes are shown at $t = 2 \times 10^9$ (non-dimensional). $f = 10^{-7}$ and $Q_0 = 0\ 5\ \ Q_1 = 0\ 99$. Each Figure was confirmed by five runs with different random initial conditions. All shapes except the one in Figure 2(f) are stationary.

The surface shown in Figure 2(f) evolves chaotically in time-space. Similar chaotic states are computed in Ref. [6], where the long wave length isothermal model is developed; there, they appear when too strong deposition destroys faceting and coarsening process induced by the strong surface energy anisotropy. Here, it is seen that the presence of the surface

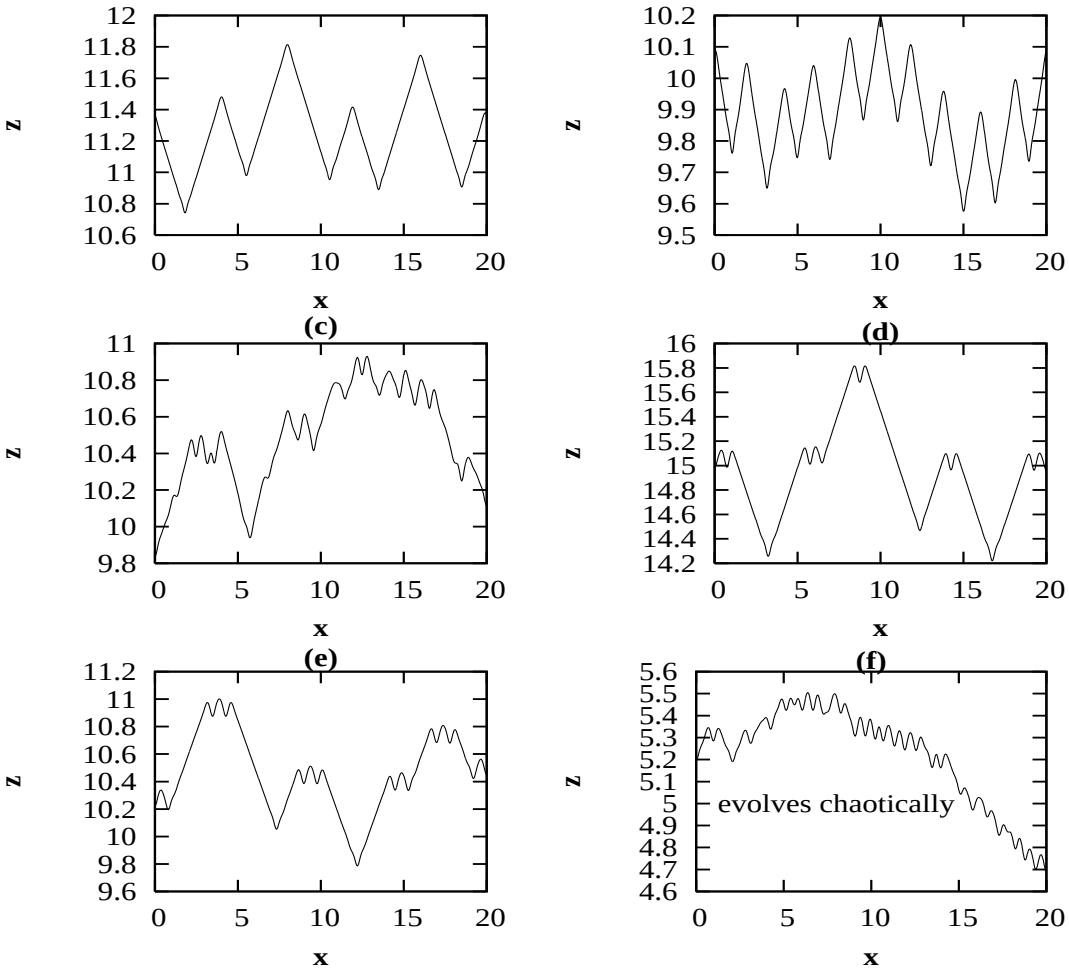

Figure 2: Surface shapes at time $t = 2 \times 10^9$ in the thermodynamically unstable case. $\bar{q} = (a)\ 0\ 25\ \ (b)\ 0\ 5\ \ (c)\ 1\ \ (d)\ 2\ \ (e)\ 4\ \ (f)\ 8$. The roughness on tops and walls of pyramids is the residual of the underlying faceting instability with wave length $\lambda_{\max} = 0\ 5$.

temperature non-uniformity inhibits the chaotic dynamics when the ratio $\bar{d}\ \lambda_{\max}$ is not too small. For the stationary pattern to emerge, the hot and cold regions may even be contained within the faceting wave length, as is the case in Figure 2(e), where $\bar{d}\ \lambda_{\max} = 0\ 5$. But when there is too many such regions within the faceting wave length, the mass transfers there destroy faceting and coarsening leading to chaos; for example, $\bar{d}\ \lambda_{\max} = 0\ 25$ in Figure 2(f). For small values of $\bar{q}$, see Figures 2(a),(b) the number of structures per length of sample is dictated by $\bar{q}$-value; in other words, the intrinsic facets coarsen in the pattern with induced wave length. However, with the increase of $\bar{q}$ (equivalently, with the decrease of $\bar{d}$ so that $\bar{d}$ $\lambda_{\max}$) the coarsening scenario changes. One observes the formation of a few (two or three) large structures which span many $\bar{d}$ and $\lambda_{\max}$ wave lengths. The morphology of these large structures is different the from sharply terminated pyramids in Figures 2(a),(b). The large structures are truncated pyramids, where the roughness on the tops and walls is the residual of the underlying faceting instability with the faceting wave length $\lambda_{\max} = 0\ 5$. Such states do not appear in the long wave length isothermal case for any value of the deposition parameter. Also note that in contrast to the just described non-isothermal arrangement, the

pyramids in the isothermal case are always separated by the faceting wave length when there is no deposition [18] or, in the presence of (weak) deposition, by the distance which reflects balance between KPZ-nonlinearity and the surface tension anisotropy causing the faceting decomposition [6].

References

[1] C. Zhang, R. Kalyanaraman, *Appl. Phys. Lett.* **83(23)**, 4827 (2003); *J. Mater. Res.* **19(2)**, 595 (2004).

[2] W. Zhang, C. Zhang, R. Kalyanaraman, *Mater. Res. Soc. Symp. Proc.* **849**, 53 (2005).

[3] C. Zhang, PhD Thesis, Dept. of Physics, Washington University, St. Louis, June 2004.

[4] J. Stewart, N. Goldenfeld, *Phys. Rev. A* **46**, 6505 (1992).

[5] F. Liu, H. Metiu, *Phys. Rev. B* **48**, 5808 (1993).

[6] T.S. Savina, A.A. Golovin, S.H. Davis, A.A. Nepomnyashchy, P.W. Voorhees, *Phys. Rev. E* **67**, 021606 (2003).

[7] W.W. Mullins, *J. Appl. Phys.* **28(3)**, 333 (1957); **30**, 77 (1959).

[8] C. Herring, in *Structure and Properties of Solid Surfaces* 5 (1952) (ed. R. Gomer and C.S. Smith, The University of Chicago Press).

[9] J.W. Cahn, J.E. Taylor, *Acta. Metall. Mater.* **42**, 1045 (1994).

[10] A. Di Carlo, M.E. Gurtin, P. Podio-Guidugli, *SIAM J. Appl. Math.* **52(4)**, 1111 (1992).

[11] A.A. Golovin, S.H. Davis, A.A. Nepomnyashchy, *Physica D* **122**, 202 (1998).

[12] B. J. Spencer, *Phys. Rev. E* **69**, 011603 (2004).

[13] M.M. Yakunkin, *High Temperatures* **26(4)**, 585 (1988).

[14] B.S. Yilbas, M. Kalyon, *J. Phys. D: Appl. Phys.* **34**, 222 (2001).

[15] M. Khenner, V.K. Henner, *J. Phys. D: Appl. Phys.* **38**, 4196 (2005).

[16] M. Khenner, Tailoring of crystal surface morphology by induced spatio-temporal oscillations of temperature , submitted.

[17] E. Hairer, G. Wanner, *J. Comput. Appl. Math.* **111**, 93 (1999).

[18] F. Hausser, A. Voigt, *Interfaces & Free Boundaries* **7(4)**, 353 (2005).